

Precise measurements the broadening characteristics and parameters of methane near-infrared absorption spectrum at high pressure

HE Ying¹, ZHANG Yu-Jun^{1,2*}, YOU Kun¹, FAN Bo-Qiang^{1,2}, LI Meng-Qi^{1,2}, YU Dong-Qi^{1,2}, XIE Hao^{1,2}, LEI Bo-En^{1,2}, JIA Wei³, JING Jun-Sen³, LIU Wen-Qing^{1,2}

(1. Key Laboratory of Environmental Optics & Technology, Anhui Institute of Optics and Fine Mechanics, Chinese Academy of Sciences, Hefei 230031, China;

2. University of Science and Technology of China, Hefei 230026, China;

3. College of Mechanical and Electrical Engineering, Anhui Jianzhu University, Hefei 230601, China)

Abstract: The high-pressure absorption spectrum at 6046.96 cm^{-1} of methane was obtained with the measurement experimental platform. The empirical mode decomposition algorithm was used to filter out the detection noise caused by window deformation at high-pressure. Consequently, the overall root-mean-square error (RMSE) of absorbance signal was reduced by 3.87 times, and the residual error of absorbance signal fitting was lower than $\pm 1\%$ by using Lorentz line-type fitting algorithm. These studies showed that the absorption line width increased with the pressure increasing, and the mutual broadening coefficient of nitrogen-methane molecules at high-pressure was calculated as 0.0631 $\text{cm}^{-1}\text{atm}^{-1}$. Moreover, the absorption line appeared a "red shift" phenomenon as the pressure increasing, and the pressure shift coefficient of nitrogen-induced was calculated as -0.00848 $\text{cm}^{-1}\text{atm}^{-1}$. Therefore, a method of concentration inversion at high pressure was proposed by the linear relationship between the detection wavelength, pressure, and pressure shift coefficient. In conclusion, the research on spectrum broadening characteristics in high-pressure environment lays foundation for spectrum detecting in industrial environment.

Key words: laser absorption spectroscopy, spectrum broadening characteristics, empirical mode decomposition algorithm, high pressure, methane, pressure shift

PACS: 42. 62. Fi, 71. 35. Cc, 42. 62. Cf, 74. 62. Fj

高压甲烷近红外吸收光谱展宽特性及参数精确测量

何莹¹, 张玉钧^{1,2*}, 尤坤¹, 范博强^{1,2}, 李梦琪^{1,2}, 余冬琪^{1,2}, 谢皓^{1,2}, 雷博恩^{1,2}, 贾巍³, 经俊森³, 刘文清^{1,2}

(1. 中国科学院环境光学与技术重点实验室, 安徽光学精密机械研究所, 安徽合肥 230031;

2. 中国科学技术大学, 安徽合肥 230026;

3. 机械与电气工程学院, 安徽建筑大学, 安徽合肥 230601)

摘要: 通过搭建的测量实验平台, 获取了甲烷 6046.96 cm^{-1} 处高压气体吸收光谱. 通过经验模态分解算法减弱了高压引起窗片形变而产生的探测噪声, 吸光度信号的均方根误差 (RMSE) 降低了 3.87 倍, 通过洛伦兹线型拟合算法获得的吸光度拟合残差优于 $\pm 1\%$. 研究表明, 谱线线宽随着压力增大而增大, 计算的高压环境的氮气-甲烷分子的互展宽系数为 0.0631 $\text{cm}^{-1}\text{atm}^{-1}$. 此外, 随着压力的增大, 吸收线出现“红移”现象, 计算得到氮气诱导压力频移系数为 -0.00848 $\text{cm}^{-1}\text{atm}^{-1}$. 由此提出一种利用检测波长、压力和压力频移系数的线性关系反演高压环境下气体浓度的算法. 总之, 高压环境下光谱展宽特性研究为工业环境下的光谱检测打下基础.

Received date: 2020-02-19, **revised date:** 2020-09-01

收稿日期: 2020-02-19, **修回日期:** 2020-09-01

Foundation items: Supported by National Natural Science Foundation of China (4180512), Key Research and Development Projects of Anhui Province (201904a07020093), Natural Science Foundation of Anhui Province (1808085MD107, 1808085QD113), Key Project of University Natural Science Research Project of Anhui Province (KJ2019A0793) and Research Project of Anhui Jianzhu University (JZ192037).

Biography: HE Ying (1983-), female, Hefei, China, associate researcher, master. The area of interest is hence gases monitoring in atmosphere with laser absorption spectroscopy. E-mail: heyings@aiofm.ac.cn

* **Corresponding author:** E-mail: yjzhang@aiofm.ac.cn

关键词: 激光吸收光谱; 光谱展宽特性; 经验模态分解算法; 甲烷; 压力频移

中图分类号: O433.1 文献标识码: A

Introduction

High-pressure gas detection is required urgently in the fields of natural gas pipeline transportation monitoring, deep submergence detection, aircraft engine diagnosis and other industries and national defense fields. Traditional semiconductor and electrochemical sensors which use contact measurement methods are prone to false alarm in high-pressure environment as the poor adaptability and difficult to meet on-line detection needs at high-pressure. In recent years, a new spectroscopy detection technology represented by Tunable Diode Laser Absorption Spectroscopy (TDLAS) technology has become a research focus in gases diagnosis under extreme conditions such as high temperature and high-pressure environment because of its high sensitivity, high selectivity, non-contact detection and strong adaptability to harsh environment^[1-3].

In high-pressure environment, due to the molecular collision aggravation the absorption spectral line broadened obviously, which led to the change of characteristic absorption spectrum. So, the spectral characteristic parameters must be accurately obtained for inverting gas concentration. At present, the study of spectral characteristic parameters at normal pressure is comprehensive. For example, Rieker *et al.*^[4] analyzed the direct absorption and second harmonic signal of CO₂ spectrum at 2 μm in high temperature and high pressure environment. Farooq *et al.*^[5] used a tunable diode laser at 2.7 μm to study the mixing and finite continuous collision effect of CO₂ absorption spectrum at high pressure. There were few studies in China, such as Ting-dong Cai^[6] adopted the spectrum modulation technology of fixed wavelength combined with the peak value of the second harmonic signal normalized with first harmonic of the CO₂ spectrum to realize the concentration measurement in high temperature and high pressure environment. Meng Sun^[7] carried out the methane measurement experiment with a 1.65 μm laser and designed a correction method of absorption lines-type in non-modulation condition. But the study on spectrum analysis algorithm and broadening characteristics at high-pressure still has a large deficiency.

As an important fuel and chemical raw material, methane has been widely used in civil and industrial fields. In this paper, the research experiment of spectrum broadening characteristics of methane at 6 046.96 cm⁻¹ in high pressure environment was carried out with TDLAS technology. Then, the high-resolution absorption spectra at different high pressures were obtained to analyze the broadening characteristics and parameters. Finally, a concentration inversion algorithm at high-pressure was designed. The research will deepen the understanding of high-resolution absorption spectrum characteristics in high-pressure environment.

1 Measurement principle

Based on Lambert-Beer's law, a monochromatic laser with the emitting frequency of ν and the initial intensity of I_0 passes through an absorption medium of L in length, and the laser intensity at the receiving end is $I_t(\nu)$, so the absorbance $A(\nu)$ used to represent the absorption intensity can be expressed as Eq. 1:

$$A(\nu) = \ln \frac{I_0(\nu)}{I_t(\nu)} = S(T)\phi(\nu)PxL \quad , \quad (1)$$

where $S(T)$ is the line strength, P is the pressure, x is the gas concentration, and $\phi(\nu)$ is normalized linear function. As the spectral frequency of molecular absorption or molecular emission is not strictly monochromatic, the molecular absorption spectrum has linewidth and line-type^[8]. In high-pressure environment, the main factor of line-type change is collision broadening which divided into Lorentz broadening and Holtsmark broadening. Collisions between molecules in excited states and other particles cause Lorentz broadening when the concentration of measured gas is low. Inelastic collisions between atoms in excited states and atoms of the same kind cause Holtsmark broadening when the concentration of measured gas is high.

Linewidth $\Delta\nu_c$ is proportional to pressure P at a certain temperature which expressed as Eq. 2:

$$\Delta\nu_c = P \sum_B x_B 2\gamma_{A-B} \quad , \quad (2)$$

where x_B is the mole fraction of collision gas, γ_{A-B} is the binary collision broadening coefficient between components B and A which is a function of temperature. Each collision pairs and specific radiation transition is corresponding to a broadening coefficient. Hitran database gives the collision broadening coefficient in the normal atmospheric environment including the self-broadening coefficient γ_{self} and the air broadening coefficient γ_{air} (at 296 K as the reference temperature, 1 atm as the reference pressure). The relationship between collision broadening coefficient $\gamma_{A-B}(T)$ and temperature T can be expressed as Eq. 3:

$$2\gamma_{A-B}(T) = 2\gamma_{A-B}(T_0) \left(\frac{T_0}{T}\right)^n \quad , \quad (3)$$

where T_0 is the reference temperature, $\gamma_{A-B}(T_0)$ is the broadening coefficient at T_0 , and n is the temperature dependent coefficient (usually < 1 , typical value is 0.5).

The center frequency of the corresponding absorption line at different pressures is obtained by linear fitting of the absorbance curves, and the corresponding relation can be expressed as Eq. 4:

$$\nu = \nu_0 + P[\delta_{N_2}(1-x) + \delta_{\text{self}}x] \quad , \quad (4)$$

where ν_0 is the original center frequency, δ_{self} is the self-induced pressure shift coefficient, and δ_{N_2} is the nitrogen-induced pressure shift coefficient.

2 Experimental equipment

The high-pressure experimental platform for spectrum detection with TDLAS was built, as shown in Fig. 1. The laser was a commercial DFB laser (NLK1U5 EAAA, NEL Corporation) with the typical center wavelength of 1 653.72 nm, the laser bandwidth of 2 MHz and the side-mode suppression ratio (SMSR) of 41.68 dB. The laser controller LDC-3724C drove and ensured the laser under stable operation, and the signal generator generated a saw-tooth signal as a wavelength scanning signal. The laser emitted and passed through a beam splitter divided the laser into two paths, wherein 98% of the laser was collimated through a stainless steel absorption cell for gas high-pressure spectrum measurement. The other 2% of the laser was collimated through an etalon for wavelength calibration and conversion from time domain to frequency domain, which was detected by a detector (GAP1000L, GPD Corporation) with the minimum noise equivalent power of 10 nW. The detection signal was transferred to a signal detection and processor for absorbance extraction and spectrum broadening characteristics analysis. The absorption cell was 100 cm in length with the pressure resistance range within 10 atm. Wedge-shaped quartz window plates are installed with a 3° inclination angle of the end face of the absorption cell to reduce the interference impact on spectrum measurement. A pressure gauge (EN837-1, Swagelok Corporation) is installed on the side wall to monitor the pressure value in whole measurement process.

3 Experiment and analysis

In this experiment, the absorption line of methane molecule at 1653.7 nm in the overtone band $2\nu_3$ was selected, and the specific parameters of methane absorption line were shown in Table 1. The typical laser linewidth is 2 MHz, and there are no strong absorption lines of interfering gases (such as water vapor, carbon dioxide, etc.) in the 0.5 nm range on both sides of the absorption line.

3.1 Experimental steps

In the experiment, the temperature and current operating parameters of the laser controller were firstly tuned to the position of the goal absorption line, and a saw-tooth signal of 100 Hz was used with the wavelength scanning range of about 0.25 nm. It is necessary to maintain air tightness in the experiment. First, 99.99% nitrogen was introduced into the high-pressure absorption cell to remove any residual gas adsorbed, and then the above

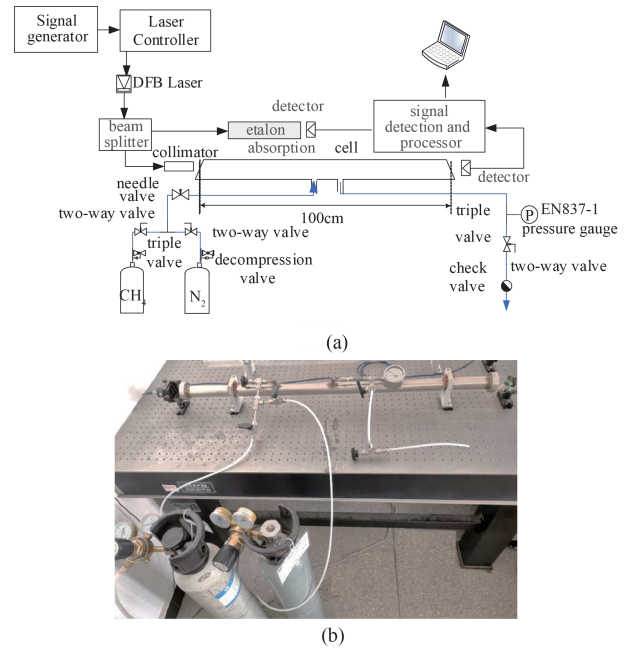


Fig. 1 (a) Spectrum measurement experimental platform, (b) gas path connection of experimental device
图1 (a) 光谱测量实验平台, (b) 实验装置气路连接

step was repeated three times with the lasting time of 2~3 minutes. Subsequently, the methane standard gas (1.0% volume concentration mixed nitrogen) was transmitted into the high-pressure absorption cell, and the valve was closed after 2 minutes. The spectrum measurement was carried out after the gas fully stabilizing about 30 seconds, and the pressure data was synchronously observed by EN837-1 gauge. Thus, a group of methane measurement spectrum was obtained respectively at different pressures (1.5~5 atm) for analyzing. The uncertainty of the standard gas used here was about 2.0% which produced by Nanjing Special Gas Corporation. The collected detection spectral signals can be converted from time domain to frequency domain by etalon signal (FSR = 3 GHz) collected synchronously.

3.2 Spectral measurement and analysis

(1) Spectrum analysis algorithm

When TDLAS technology was used to gas detection, the noise caused by electronic components, window deformation in high-pressure environment and other factors will affect the measurement accuracy. Therefore, according to the non-linear and non-stationary characteristics of spectral signals, the empirical mode decomposition algorithm was selected to filter the detected spectral signals

Table 1 Specific parameters of methane absorption line at 6046.9647 cm^{-1} (Hitran2008 database)

表1 甲烷6 046.964 7 cm^{-1} 吸收线参数(Hitran2008数据库)

Specific parameters	Value
spectral line intensity $S(\text{cm mol}^{-1})$	1.34E-21
air-broadened half width at half maximum $\gamma_{\text{air}}@296 \text{ K} / (\text{cm}^{-1} \text{ atm}^{-1})$	0.062 1
self-broadened half width at half maximum $\gamma_{\text{self}}@296 \text{ K} / (\text{cm}^{-1} \text{ atm}^{-1})$	0.082
temperature dependence coefficient of the air-broadened n	0.85
pressure shift of the air-broadened $\delta_{\text{air}}@296 \text{ K} / (\text{cm}^{-1} \text{ atm}^{-1})$	0

according to the advantages and disadvantages of various de-noising algorithms. Then, the Lorentz line-type fitting algorithm was used to obtain the absorbance signal and extract the characteristic absorption spectrum. The spectral analysis algorithm was as follows^[9-10]:

(i) Firstly, all the extreme points in the specific signal $X(t)$ were founded out, then, the upper envelope and the lower envelope were formed by cubic spline curve method with all of the extreme points. Supposing the average value of the upper and lower envelopes were m_1 , and the difference H_1 can be expressed as Eq. 5:

$$H_1 = X(t) - m_1 \quad (5)$$

At the same time, H_1 was regarded as a new $X(t)$, and the above steps were repeated until H_1 satisfying the two conditions of the eigenmode function IMF . Then H_1 was defined as the first-order IMF , denoted as IMF_1 . In general, the highest frequency component of the original signal was located in IMF_1 .

(ii) Secondly, the IMF_1 was separated from $X(t)$ to obtain the difference signal r_1 which was expressed as Eq. 6:

$$r_1 = X(t) - IMF_1 \quad (6)$$

where r_1 was regarded as a new signal and the above steps were also repeated until the residual signal of the n order became a monotone function when the IMF variables which satisfied the eigenmode function cannot be generated. The residual signal of the n order was regarded as Eq. 7:

$$r_n = r_{n-1} - IMF_n \quad (7)$$

Mathematically, $X(t)$ can be expressed as the sum of IMF components and a residual function, i. e. :

$$X(t) = \sum_{j=1}^n IMF_j(t) + r_n(t) \quad (8)$$

where $r_n(t)$ was the residual function representing the average trend which contained different frequencies components arranged from high to low.

(iii) Thirdly, the IMF of each order was separated by a preset threshold value to generate the de-noised IMF components which were accumulated together with the residual function and to realize the de-noised signal reconstruction.

(iv) The de-noised signal was subjected to background baseline fitting to extract the absorbance signal. In general, the signal de-noising effect is evaluated by the signal-to-noise ratio (SNR) or root-mean-square error (RMSE)^[11]. The overall RMSE of the original absorbance signal and the de-noised absorbance signal were calculated respectively, and it was reduced by 3.87 times after de-noising, as shown in Fig. 2(a).

(v) The Lorentz line-type function was used to fit absorbance spectral signal after time domain to frequency domain converting, and the fitting residual error was calculated within $\pm 1\%$, as shown in Fig. 2(b).

(2) Measurement of N_2 - CH_4 mutual broadening coefficient

A group of spectral signals at different pressures were measured. The absorption linewidth showed obvious broadening characteristics that it increased with pressure increasing but the peak values of the signals decreased, so the line shape tended to be flat. The integrat-

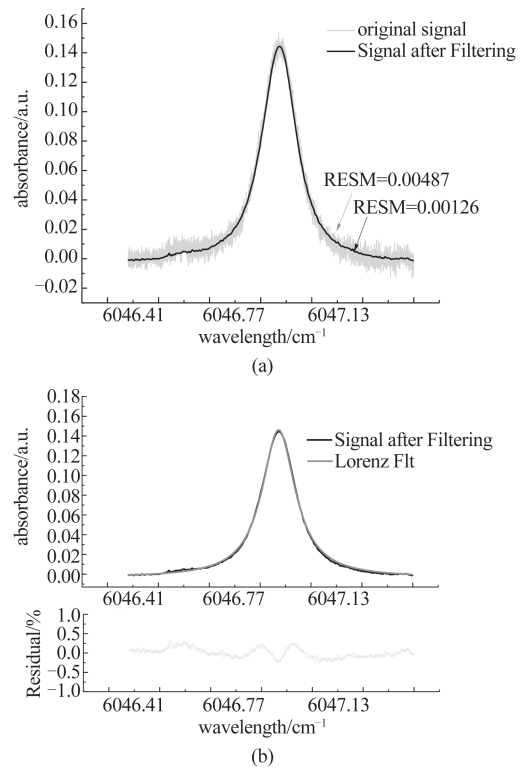


Fig. 2 (a) Absorbance signal before and after filtering, (b) line-type fitting and residual result
图2 (a)滤波前后的吸光度信号, (b)线型拟合和残差结果

ed absorbance spectral signals were shown in Fig. 3, in which the linewidth increased from 0.19 cm^{-1} at 1.5 atm to 0.62 cm^{-1} at 5 atm .

The line-type change of gas absorption lines was mainly due to the gas molecule collision intensifying in high pressure environment which enhanced the collision broadening effect. The actual broadening coefficient of absorption line was obtained by calculating the slope of linear fitting of the line-width result at different pressures, as shown in Fig. 4. The slope $k(T)$ can be expressed as Eq. 9:

$$k(T) = 2\gamma_{\text{self}}(T)x_{\text{CH}_4} + 2\gamma_{\text{N}_2-\text{CH}_4}(T)(1 - x_{\text{CH}_4}) \quad (9)$$

In this experiment, the methane concentration was 1.0% , so the content of N_2 molecules in unit volume was much larger than that of methane molecules. Therefore, self-broadening caused by collision between the same molecules can be ignored, only the nitrogen broadening of the collision between methane molecules in excited state and N_2 molecules needed to be considered. The nitrogen broadening coefficient was calculated to be $0.0624 \text{ cm}^{-1}\text{atm}^{-1}$ at high pressure, which was slightly higher than the air broadening coefficient in Hitran database.

(3) Measurement of pressure shift coefficient of nitrogen-induced

A group of center frequency of absorption line at different pressures was obtained by linear fitting of absorbance signals, as shown in Fig. 5. It was seen that the absorption line moved to the long wave direction with pressure increasing, i. e. , that is the "red shift" phenom-

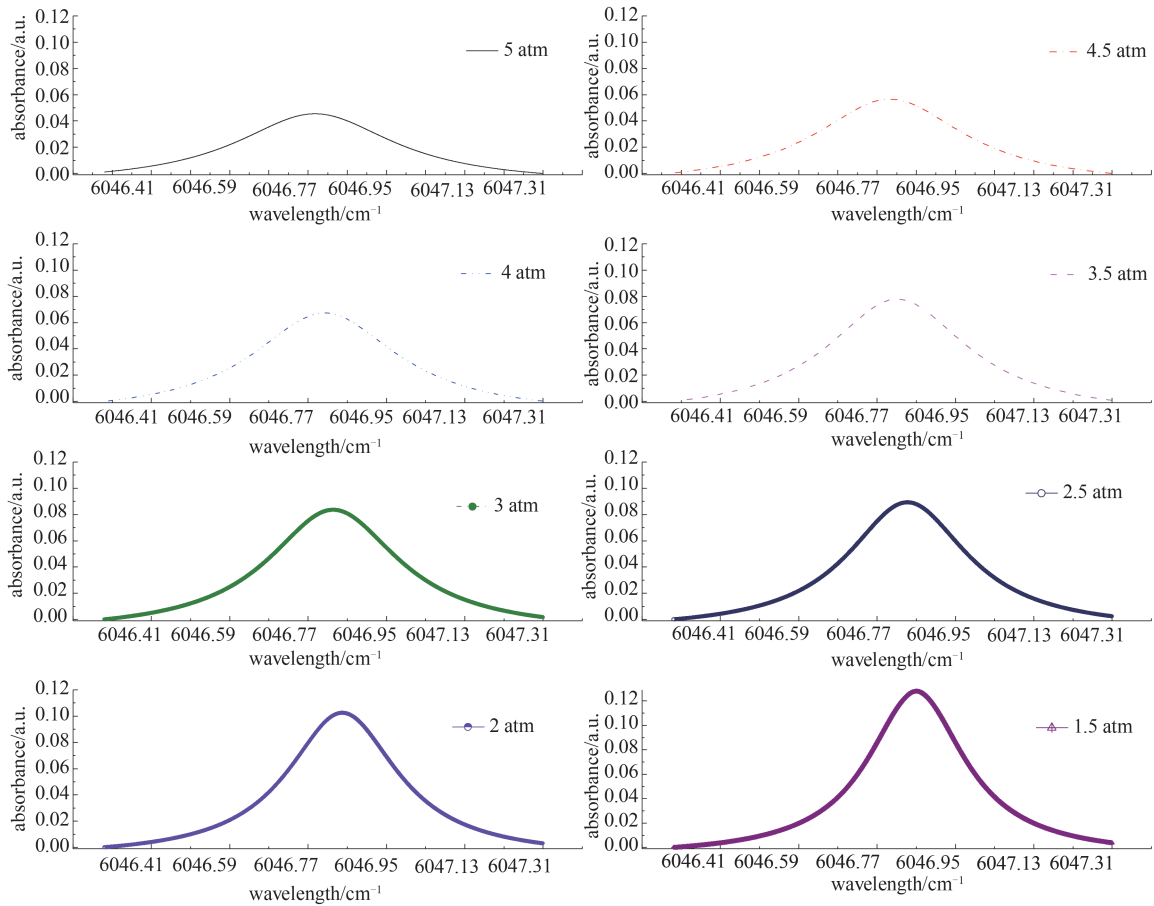


Fig. 3 Absorbance spectral signals after Lorentz line-type fitting
图3 洛伦兹线型拟合后的吸光度光谱信号

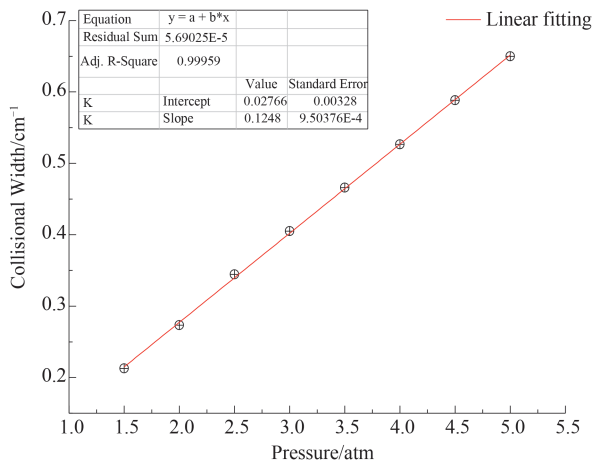


Fig. 4 Nitrogen broadening coefficient at 6 046.96 cm⁻¹
图4 6 046.96 cm⁻¹处的氮气展宽系数

enon. On the contrary, the center wavelength corresponding to the absorption peak shifted to the short-wave direction as the pressure decreasing, which is called "blue shift" phenomenon. There was a good linear relationship between the center frequency and the pressure. The intercept as the center frequency in experiment was 6 046.963 8 cm⁻¹, which can be expressed as Eq. 10. The slope as the pressure shift coefficient of nitrogen-in-

duced was calculated as -0.00848 cm⁻¹atm⁻¹ at high pressure, which does not exist in the Hitran database.

$$\nu = 6\,046.963\,8 - 0.008\,48 \cdot P(1 - x) \quad (10)$$

According to the above analysis, the unknown low concentration x can be measured as Eq. 11 when the frequency corresponding to the peak value of the absor-

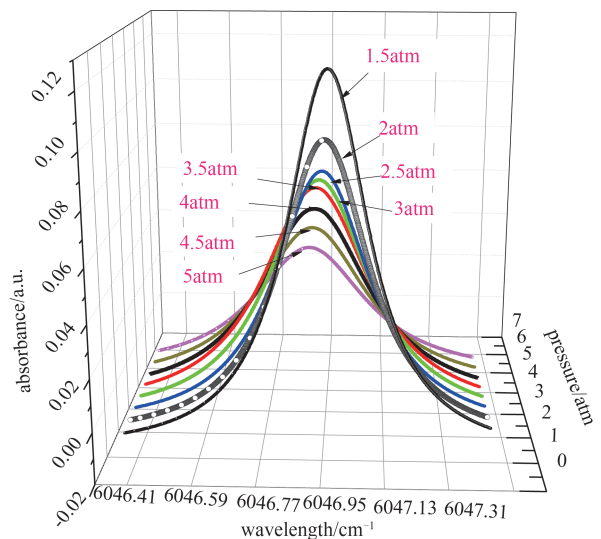


Fig. 5 Center frequency drift phenomenon
图5 中心频率漂移现象

bance signal and the current pressure were known:

$$x = 1 - \frac{6046.9638 - \nu}{0.00848P} \quad (11)$$

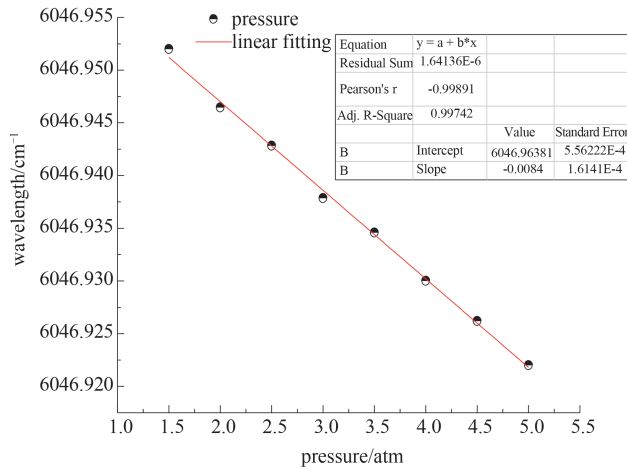


Fig. 6 Calculated the pressure shift coefficient of nitrogen-induced

图6 计算的氮气诱导压力频移系数

In TDLAS system, the amplitude of the wavelength scanning signal was within a certain range to ensure the normal operation of the laser. As the pressure increased, the absorption signal linewidth had gradually increased, while the proportion of the directly detected signal without absorption part gradually decreased. Therefore, Lorentz line-type fitting results of absorbance signal were incomplete (as shown of dotted line in Fig. 7) which results in the concentration inversion deviation augment.

In the experiment, a group of methane standard gases with different concentrations were transported into the high-pressure absorption cell, and the absorbance signals after air pressure stabilizing were obtained as shown in Fig. 7. The gas concentration can be inverted according to Eq. 11 with the center frequency of absorption signal and the pressure, that the maximum relative error of 0.2% methane concentration was calculated as 4.0%, as shown in Table 2. This method provided another method for concentration inversion in the condition of absorbance signals severe broadening at high pressure.

4 Conclusions

In Conclusion, the methane absorption spectrum at 6046.96 cm⁻¹ in high-pressure environment was measured with a spectrum detection platform by optimally extracting absorbance signals through empirical mode decomposition algorithm filtering and Lorentz line-type fitting. Then, the broadening characteristics of methane absorption spectrum at high pressure were studied. These studies show that the peak value of absorbance decreased and the linewidth increased with the pressure increasing. The methane-nitrogen mutual broadening coefficient measured at high pressure was about 0.0624 cm⁻¹atm⁻¹, slightly higher than the air broadening coefficient in Hitran database. The pressure shift coefficient of nitrogen-induced

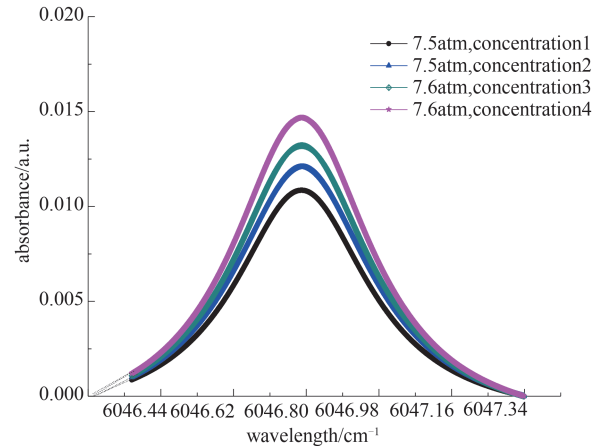


Fig. 7 Absorbance signals of different concentration at high pressure

图7 不同浓度的高压下吸光度信号

Table 2 Methane standard gas concentration and inverted concentration

表2 甲烷标气浓度与反演浓度结果

Time	Ture concentra- tion/(%)	Inverted concen- tration/(%)	Relative error /(%)
1	0.500	0.512	2.40
2	0.400	0.390	2.50
3	0.300	0.311	3.67
4	0.200	0.208	4.00

under high pressure was -0.0084 cm⁻¹atm⁻¹, which was not listed in Hitran database. The gas concentration can be inverted by measuring center frequency of absorption line when the absorbance cannot be effectively obtained in higher pressure condition with the corresponding relationship between the pressure shift coefficient of nitrogen-induced, gas concentration, center frequency and pressure. At the same time, the feasibility of the experimental system and spectrum processing algorithm was verified, which laid a foundation for subsequent research on gas spectral characteristics at high pressure.

References

- [1] Aoyagi Y, Osada H, Misawa M, *et al.* Advanced diesel combustion using of wide range, high boosted and cooled EGR system by single cylinder engine[C].SAE Technical Paper, 2006, 2006-01-0077.
- [2] Pantani M, Castagnoli F, D'Amato F, *et al.* Two infrared laser spectrometers for the in situ measurement of stratospheric gas concentration[J]. *Infrared physics & technology*, 2004, **46**(1): 109-113.
- [3] Roller C, Namjou K, Jeffers J, *et al.* Simultaneous NO and CO₂ measurement in human breath with a single IV-VI mid-infrared laser [J]. *Optics letters*, 2002, **27**(2): 107-109.
- [4] Rieker G B, Jeffries J B, Hanson R K. Calibration-free wavelength modulation spectroscopy for measurements of gas temperature and concentration in harsh environments [J]. *Applied Optics*, 2009, **48**(29): 5546-5560.
- [5] Farooq A, Jeffries J, Hanson R. High-pressure measurements of CO₂ absorption near 2.7 μm: Line mixing and finite duration collision effects [J]. *Journal of Quantitative Apectroscopy and Radiative Transfer*, 2010, **111**: 949.
- [6] CAI Ting-Dong, GAO Guang-Zhen, WANG Min-Rui, *et al.* Measurements of CO₂ concentration at high temperature and pressure environment using Tunable Diode Laser Absorption Spectroscopy [J]. *Spectroscopy and Spectral Analysis*(蔡廷栋,高光珍,王敏锐,等.高

- 温高压下基于TDLAS的二氧化碳浓度测量方法研究. *光谱学与光谱分析*, 2014, **34**(7):1769-1773.
- [7] SUN Meng. The absorption line-shapes recovery research of gas detection system based on TDLAS[D]. Shan Dong University, Thesis for Master Degree(孙猛.基于TDLAS技术气体检测的理论模型修正研究.山东大学硕士学位论文),2014:31-44.
- [8] Michopoulos P, Baloutsos G, Economou A, *et al.* Effects of nitrogen deposition on nitrogen cycling in an Aleppo pine stand in Athens, Greece[J]. *Science of the Total Environment*, 2004,**323**: 211-218.
- [9] Huang N E, Shen Z, Long S R, *et al.* The empirical mode decomposition and the Hilbert spectrum for nonlinear and non-stationary time series analysis [J]. *Proceedings of the Royal Society*, 1998, **454** (1971): 903-995.
- [10] JIA Wei, HE Ying, ZHANG Yu-Jun, *et al.* Spectral analysis and line strength measurement method of near-infrared overlapped absorption lines[J]. *Journal of Infrared and Millimeter Waves*(贾巍,何莹,张玉钧,等.近红外混叠吸收线光谱解析及线强测量方法研究. *红外与毫米波学报*),2018,**37**(1):106-111.
- [11] Li J S, Yu B L, Fischer H. Wavelet transform based on the optimal wavelet pairs for tunable diode laser absorption spectroscopy signal processing[J]. *Applied Spectroscopy*, 2015, **69**(4):496-506.